*J Mater Sci* (2020) 55:2405–2418

Composites & nanocomposites

# Silica aerogel-integrated nonwoven protective fabrics for chemical and thermal protection and thermophysiological wear comfort

M. A. Rahman Bhuiyan[1], Lijing Wang[1,*], Abu Shaid[1], Israt Jahan[1], and Robert A. Shanks[1]

[1] School of Fashion and Textiles, RMIT University, 25 Dawson Street, Brunswick, Melbourne, VIC 3056, Australia

**Received:** 11 August 2019
**Accepted:** 7 November 2019
**Published online:** 15 November 2019



## ABSTRACT

This research has designed and prepared a protective clothing layer by integrating porous silica aerogel with nonwoven fabrics for simultaneous chemical and thermal protection. Protective interlining having resistance to heat and liquid chemical penetration was developed by sandwiching randomly distributed aerogel particles between viscose nonwoven fabric layers. The nonwoven layer and aerogel particle layer were explored by analysing fabric surface morphology. Physical characterization of the test specimens revealed that the weight and thickness of fabric increased after the integration of aerogel particles. Consequently, improved chemical resistance and thermal resistance were observed in the aerogel–nonwoven fabrics with higher aerogel concentration. For clothing comfort, the high air permeability indicated sufficient breathability by transferring air and water vapour from the body to the atmosphere and vice versa through apparel. Improved evaporative transmittance and cooling index of aerogel–fabrics suggested that the fabric will create a favourable thermal comfort microenvironment between the skin and apparel. For wear comfort regarding wet clinginess, the high water uptake and evaporation rate of the fabric specimens indicated their ability to retain and evaporate large amounts of perspiration vapour in a hot and humid atmosphere. The overall performance of the aerogel–nonwoven fabrics suggested that the integration of silica aerogel with viscose nonwoven fabric is a prospective approach for developing protective interlining that will provide reliable chemical and thermal protection as well as adequate clothing comfort to the wearer.

Address correspondence to E-mail: lijing.wang@rmit.edu.au

https://doi.org/10.1007/s10853-019-04203-2

## Introduction

Silica aerogel is a lightweight porous material derived from a gel, in which the liquid component is confined in three-dimensional porous networks, and replaced with a gas [1]. It is an extremely low-density material with the lowest bulk density (~ 0.003 g/cm$^3$) compared with any known porous solid [2]. This low bulkiness is attributed to its highly porous structure. The porosity is as high as 99.0% with different pore sizes, such as micropores (< 2 nm), mesopores (2 to 50 nm), and macropores (> 50 nm) [3]. Silica aerogel possesses some unusual characteristics including high specific surface area (500–1000 m$^2$/g) [4], impressively high thermal insulation value (~ 13 mW/m K) [5], ultra-low dielectric constant ($k$ = 1.0–2.0) [3], and excellent hydrophobicity. Silica aerogel has gained considerable attention for various applications, including acoustic insulation [6], electrical batteries [7, 8], water air purification [9], and so forth. However, this material is extremely fragile due to its high porosity and cracking, which creates some difficulties for its widespread conventional applications [10]. Hence, the integration of aerogels with a porous textile structure, including woven and nonwoven, can be considered an easy and effective approach through filling the interstitial space among fibres within the structure. Early research on aerogels in the field of textiles was based on the development of spacesuit insulation, funded by NASA [11]. Recent application examples included silica aerogel coating on wool–aramid blended fabric for thermophysiological wear comfort [12], aerogel-encapsulated nonwoven textiles for thermal insulation [10], and polyester/polyethylene nonwoven blankets with aerogel for extreme cold weather [13]. In addition, several contemporary research studies explored the prospect of using silica aerogel as a thermal liner in fire-protective garments [14, 15]. All the research activities revealed that the incorporation of silica aerogel with the textile structure could significantly improve the thermal performance of the composite material. However, minimal literature has discussed the application of silica aerogel in protective clothing for chemical protection. Recently, silica aerogel-incorporated polyurethane (PU) coating on the cotton fabric surface was developed for simultaneous chemical protection and thermal comfort [16]. Since the coating of aerogel with PU binder filled into the porous space of the loose textile structure partially or entirely, several limitations of the coated fabric, for instance high stiffness and bulkiness, as well as low moisture vapour permeability, were reported.

Nonwoven fabrics are generally sheet, web, or batts of entangled fibres, orientated directionally or randomly, bonded together by various methods including mechanical, thermal, and chemical [17]. Unlike other textile structures, for example knitted or woven, the construction of nonwoven fabric consists of individual fibres or layers of fibrous webs rather than yarns [18]. The unique structural features of nonwoven fabrics lead some exceptional functional characteristics, such as high resilience, great compressional resistance, as well as excellent thermal-insulating properties [19]. Besides, the nonwoven structure is highly porous, low weight, and permeable, which can be utilized to develop lightweight clothing with adequate breathability for clothing comfort. Therefore, nonwoven fabrics are extensively used in various technical applications, including protective clothing materials.

Protective clothing is generally intended to create reliable protection against hazardous materials and the environment, as well as lowering the risk of injury or illness of the wearer [20]. Designing any protective fabric having maximum protection with the best possible wear comfort is two contradictory aspects that are difficult to obtain in any protective clothing system [21]. In this regard, the use of nonwoven fabric as interlining (the fabric used between the inner and outer layers of a garment) is a prospective approach to design barrier clothing having permeability to air and moisture vapour. The integration of porous silica aerogel with a nonwoven fabric can be employed to provide chemical protection, through liquid chemical adsorption within the minute pores of the particles. The aerogel particles are anticipated to enhance the chemical adsorption due to their open-pore network. The open-pore structure and the interconnectivity of the pores within the particles facilitate the chemical adsorption through flowing the liquids from one pore to another [16]. In addition, the low thermal conductivity of silica aerogel along with high air entrapping potential of flexible porous nonwoven can be utilized to develop high thermal resistant aerogel–nonwoven composites. Therefore, silica aerogel-integrated nonwoven fabric is expected to provide simultaneous

chemical and thermal protection with no declining thermophysiological wear comfort.

The aim of this research is to design and develop a protective interlining by incorporating silica aerogel particles within the nonwoven fabric for simultaneous chemical and thermal protection along with acceptable comfortability. Performance is assessed by investigating the radiant heat and liquid chemical resistance, as well as the clothing comfort in terms of air permeability, thermal and evaporative resistance, and moisture evaporation rate of the newly developed fabrics.

## Experimental

### Materials

Viscose staple fibre from Tianjin Glory Tang Fiber Technology Co., Ltd., China, was used as the raw material of nonwoven fabrics. Low melting temperature solid polyester staple fibre from Shanghai Polytex Co., Ltd., China, was employed for thermal bonding of fabric. The representative parameters and values of both the viscose and polyester fibres are shown in Table 1.

Enova silica aerogel (IC3120) was procured from Cabot Corporation, USA, and used as received. The aerogel was hydrophobic solid powder having size 100–1200 μm with particle density 120–150 kg/m$^3$ and pore diameter ~ 20 nm. Chemical resistance of fabric was assessed with organic chemicals from Chem-Supply Pty Ltd., Australia (acetone, methanol, *N*, *N*-dimethylformamide (DMF), toluene, and ethyl acetate), Sigma–Aldrich Pty Ltd., Australia (*n*-hexane), and BDH Chemicals Ltd., England (acetonitrile), respectively.

## Methods

### Development of nonwoven fabric

The nonwoven fabric for interlining in protective clothing was developed using the viscose and polyester staple fibres listed in Table 1. Viscose fibre was used to enhance the water/moisture vapour absorption due to its hydrophilic nature as well as high water absorption capacity (moisture regain of 11.5%) [22]. The low melting temperature polyester fibre was employed for thermal bonding of viscose fibres within the fabric by heat setting.

Viscose and polyester fibres were mixed at the ratio of 80:20 to obtain satisfactory thermal bonding of fibres in the fabric. The fibre mixture was fed to a carding machine (Shin Chang carding machine from Shin Chang Industry Co., Ltd., Taiwan) to produce a dry-laid web. Hereafter, heat setting was carried out on the web at a temperature of 140 °C and a pressure of 6.0 kPa for 3 min using a Magic stream press 7 (MSP7) from Singer. Finally, aerogel particles of different amounts such as 1.0, 2.0, 3.0, and 4.0 g were dusted precisely through a perforated tumbler on one layer of the nonwoven fabric (30 cm × 30 cm). To prevent any unexpected leaking of aerogel particles from the fabric edges and increase thermal bonding in the case of higher aerogel concentrations (3.0 and 4.0 g), a fusible interlining was employed to firmly secure the particles and fabric edges. Another layer of the nonwoven fabric covered the layer with aerogel particles. An aerogel-integrated sandwich structure was then formed by heat press. The manufacturing process of aerogel–nonwoven fabric is shown schematically in Fig. 1.

The experimental investigation was conducted using four types of specimen prepared by adding aerogel particles as mentioned above, including 1.0, 2.0, 3.0, and 4.0 g, which were coded as NA1, NA2, NA3, and NA4, respectively. Nonwoven control fabric (NC) was made without adding aerogel. The

**Table 1** Specifications of viscose and polyester fibres

| Viscose fibre | | Polyester fibre | |
|---|---|---|---|
| Fineness | 1.5 D | Fineness | 4.0 D |
| Fibre length | 38 mm | Fibre length | 51 mm |
| Fibre type | Staple fibre | Fibre type | Low melt staple fibre |
| Colour | Red | Colour | Raw white |
| Grade | 100% virgin | Melting temperature | 110 °C |

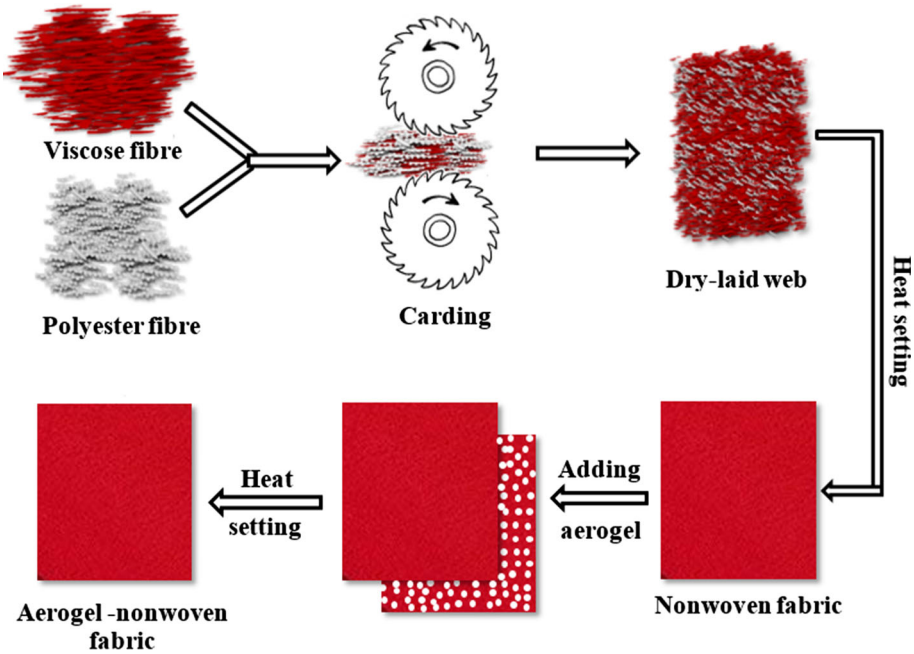


**Figure 1** Schematics of method for developing nonwoven fabric.

protective performance of aerogel–nonwoven fabrics was compared with a commercial chemical protective clothing fabric (CC). The CC fabric comprised of three layers, including a hydrophobic outer shell fabric, activated carbon fabric in the inner layer, and cotton fabric directly in contact with the body skin. A detailed construction of this commercial protective clothing has been discussed in our previous paper [20].

## Fabric characterization and evaluation

### *Fabric morphology*

Fabric morphological analysis was conducted using field-emission scanning electron microscopy (FE-SEM, Quanta$^{TM}$-200, UK) in a low vacuum mode at an accelerating voltage of 30 kV. Prior to the SEM analysis, a dual-action sputter coating machine (Precision etching coating system, Gatan-682) was employed to produce a thin platinum layer on the fabric surface.

### *Fabric thickness and weight*

The thickness of fabric specimens was determined according to the standard ASTM D1777–15 using a fabric thickness tester. Besides, the weight per unit area (GSM) of fabric was measured following ASTM D3776-96 standard.

### *Chemical adsorption*

The test for the chemical adsorption capacity of the experimental fabrics was carried out by using seven liquid chemicals of different surface tension. The chemicals were selected following ASTM F1001-12. The chemicals and their respective surface tension value are listed in Table 2.

During the experiment, a fabric specimen of 6.45 cm$^2$ was placed on a smooth and horizontal surface of a petri dish. Then, each liquid was dropped from a fixed position (above 10 cm above fabric surface) to a specific point on the fabric continuously at a constant rate (30 drops/min) until penetrating through the fabric. The chemical adsorption was calculated from the mass of fabric following Eq. 1,

**Table 2** Liquid chemicals and their surface tension for chemical adsorption testing

| Chemical | Surface tension (dyne cm$^{-1}$) at 20 °C |
|---|---|
| Dimethylformamide | 37.10 |
| Acetonitrile | 29.10 |
| Toluene | 28.52 |
| Acetone | 25.20 |
| Ethyl acetate | 23.20 |
| Methanol | 22.50 |
| *n*-Hexane | 18.43 |

and the results for three specimens of each test fabric were averaged.

$$\text{Chemical adsorption}(\%) = \frac{m_2 - m_1}{m_1} \times 100 \quad (1)$$

where $m_1$ and $m_2$ are the mass of fabric before and after chemical adsorption, respectively.

### Resistance to chemical penetration

The resistance of test specimens against chemical penetration was assessed by following BS ISO 22608:2004. The chemical resistance was evaluated in terms of repellency, retention, and penetration of the liquid chemical through the fabric. The detailed procedure for the measurement of the proportion of repellency, retention, and penetration of the liquid chemicals was mentioned in our previous report [21].

### Thermal resistance

The fabric thermal resistance measurement was conducted according to ISO 11092:2014 using the integrated sweating hotplate (Model 431-213, Measurement Technology Northwest, USA). Standard test conditions including 20.0 ± 0.1 °C ambient temperature, 35.0 ± 0.1 °C thermal guard temperature, 1.00 ± 0.05 m/s of airspeed, and 65.0 ± 3.0% RH inside the test chamber were maintained throughout the experiment. At the steady-state condition of the system, the thermal resistance of the fabric was calculated from Eq. 2.

$$R_{cf} = R_{ct} - R_{cb} = \frac{A(T_s - T_a)}{H - \Delta H_c} - R_{cb} \quad (2)$$

where $R_{cf}$ is the actual thermal resistance provided by the fabric alone ($m^2$ °C/W); $R_{ct}$ is the total thermal resistance of the system including fabric and air layer ($m^2$ °C/W); $R_{cb}$ is the bare plate thermal resistance ($m^2$ °C/W); $A$ is the hot plate area ($m^2$); $T_a$ and $T_s$ are the ambient and surface air temperature (°C), respectively; $H$ is the power input to the hot plate; $\Delta H_c$ is the correction factor.

The thermal imaging of the selected test specimens, including NC, NA4, and CC, was performed by using a FLIR T400-series infrared camera. A constant temperature of 35.0 ± 0.1 °C of the guard hot plate was maintained to provide fabric sample a uniform thermal condition. The ambient temperature of the chamber was kept 20.0 ± 0.1 °C throughout the experiment. The change of fabric surface temperature was recorded by the infrared thermal camera at a distance of 40 cm, and images were taken over 90 s.

### Radiant heat resistance

The radiative heat resistance of test specimens was assessed using a bench-scale test apparatus. This instrument was employed to measure the radiant heat resistance of textile materials in several earlier studies [15, 23, 24]. The development of this apparatus and the detailed test procedure has been described by Shaid et al. [25]. During the experiment, the fabric specimens were subjected to a radiant heat source (250 °C) from a distance of 15 cm. The rise of temperature behind the exposed fabric was measured by heat sensors in every 2 s and recorded with an open-source data logging software '*Tera Term*'. Then, the time to reach 44 °C (pain threshold) and 55 °C (second-degree burn temperature) was recorded from the time–temperature readings of each fabric specimen. Finally, these readings were analysed to compare the radiative heat resistance of the fabrics.

### Air permeability

The breathability concerning the air permeability of fabric specimens was measured according to EN ISO 9237:1995. The test was performed using SDL Atlas air permeability tester (M021S, SDL Atlas Pty Ltd., England). The specimen was clipped over the air inlet orifice (working area = 5.0 $cm^2$ ± 0.5%) and tested at a constant pressure of 100 Pa. The mean air permeability was calculated from the airflow readings (mL $cm^{-2}$ $s^{-1}$) of five specimens from each fabric tested.

### Evaporative resistance and permeability index

Evaporative resistance of experimental fabrics was assessed according to the ISO 11092:2014 standard. The experiment was conducted using the same instrument and procedure as mentioned earlier for the thermal resistance test. However, both the thermal guard and air temperature were maintained at 35 ± 0.1 °C and the test chamber at 40 ± 3% RH for evaporative resistance. The evaporative resistance provided by the fabric under the steady-state condition was determined by using Eq. 3.

$$R_{ef} = R_{et} - R_{eb} = \frac{A(P_s - P_a)}{H - \Delta H_e} - R_{eb} \quad (3)$$

where $R_{et}$ is the total evaporative resistance provided by the system including fabric and air layer (Pa $m^2$/W); $R_{ef}$ is the fabric evaporative resistance (Pa $m^2$/W); $R_{eb}$ is the evaporative resistance of the air layer, i.e., bare plate (Pa $m^2$/W); $A$ is the hot plate area ($m^2$); $P_s$ is the water vapour pressure on the measuring unit surface (Pa); $P_a$ is water vapour pressure of the air (Pa); $H$ is the power input to the plate; $\Delta H_e$ is the correction factor.

The moisture permeability index ($i_{mt}$) is generally used to determine the degree of evaporative cooling of fabric. It was calculated from the average of dry heat and evaporative resistance of each test fabrics by Eq. 4.

$$i_{mt} = K\left(\frac{R_{ct}}{R_{et}}\right) \quad (4)$$

where $K$ is a constant having the value of 60.6515 Pa/°C.

### *Water uptake and evaporation rate of fabric*

The water uptake and evaporation rate of fabric were assessed according to the procedure described by Houshyar et al. [26]. Each conditioned fabric specimen (weight, $w_1$) having size 10 cm × 10 cm was dipped in the distilled water (20 ± 1 °C) for 5 min and allowed 1 min to drip the excess water on the fabric after removing it from the distilled water. Then, the fabric weight ($w_2$) was measured, and the fraction of water uptake was calculated using Eq. 5.

$$\text{Water uptake}(\%) = \frac{w_2 - w_1}{w_1} \times 100 \quad (5)$$

The water evaporation rate of fabric was determined by removing the excess amount of distilled water from the saturated fabric by padding. The specimens after pad-dried were kept flat in the standard atmospheric condition of 65 ± 2% RH and 20 ± 2 °C and allowed them to gain standard regain through evaporating the water. The evaporation rate in terms of reduction of water content in fabric was calculated at the constant time intervals of 60, 120, 180, 240, 300, 360, 420, 480, and 540 min.

## Results and discussion

### Fabric morphology

The morphology of nonwoven fabric and the distribution of aerogel particles within the fabric was examined by scanning electron microscopy. The dispersed aerogel particles on one layer of fabric were exposed after removing another nonwoven layer and investigated through creating images at different magnifications.

The SEM micrographs in Fig. 2a showed viscose fibrous materials along with their random distribution in the fabric. Besides, the porous structure of the nonwoven specimen indicates that the fabric should have good permeability to air and moisture vapour. This porous structure also suggests the loftiness or fullness of the nonwoven fabric. In the case aerogel-integrated fabrics (Fig. 2b), it was observed that most of the pores in the fabric were covered by the aerogel particles, which were distributed randomly among the fibres in the fabric. As porous silica aerogel particles are very low density materials, a mass of particles can cover a large surface area. Therefore, a layer of particles is shown in the SEM images of aerogel-incorporated nonwoven fabric. Silica aerogel is fragile, and there is a possibility of the breakage of particles due to the 6.0 kPa pressure applied. However, the soft pressing surface and the loftiness or fullness of nonwoven fabrics, as well as their porous structure, are unlikely to cause significant particle breakage as revealed in Fig. 2b. Regardless, particle breakage, if there was any, would not affect aerogel–nonwoven fabrics thermal and protection performance, which was governed by the aerogel amount.

### Thickness and weight of the fabric

The thickness and weight of the specimens including commercial and nonwoven fabrics are presented in Fig. 3. The commercial fabric had a minimum thickness among all the specimens. However, nonwoven fabrics were much lighter compared with their commercial counterpart though they are thicker than the commercial fabric. This was due to the porous structure of nonwoven fabrics consisting of individual fibres or layers of fibrous webs that creates the loftiness or fullness of the fabric. Besides, the aerogel particles in the fabric further increase the fabric thickness. In addition, the nonwoven structure is

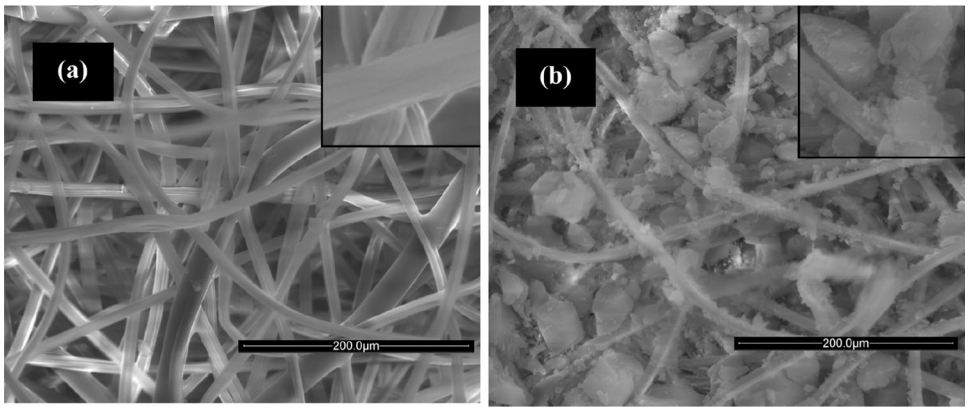


**Figure 2** SEM micrographs of **a** nonwoven fabric without aerogel and **b** aerogel-incorporated nonwoven fabrics (NA4). Insets: detailed views.

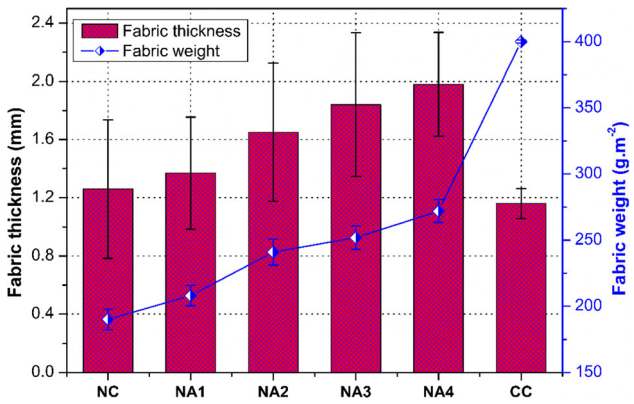


**Figure 3** Change of fabric weight and thickness of nonwoven specimens after addition of aerogels.

characteristically not uniform in either fabric thickness and weight or both [18] and therefore exhibited a greater standard deviation (SD), as revealed in Fig. 3.

In the case of fabric weight, compared with the commercial clothing weight (400 g $m^{-2}$), a considerable decrease in weight (190 g $m^{-2}$) was observed for the control nonwoven specimen. The weight of aerogel–nonwoven fabrics increased gradually with the increment of aerogel particles. As mentioned earlier, the structure of nonwoven has air gaps among the fibres. Due to the porous structure, the thickness of the fabric increased substantially without affecting the weight significantly. This low weight of fabrics can be utilized to develop lightweight protective clothing having less weight burden on the body of the user.

## Liquid chemical adsorption

The liquid chemical adsorption capacity concerning the chemical protection performance of test fabrics is shown in Fig. 4. Since the chemical resistance was assessed by the amount of liquid chemical adsorption, it can be predicted that more protection will be provided when adsorbing more liquid.

Figure 4a shows the change of chemical adsorption with the increment of aerogel concentration in the fabric. The maximum liquid adsorption among all the specimens was observed for the fabric NA4, having aerogel content 4.0 g. The commercial fabric also demonstrated a considerable amount of chemical adsorption, which is between the specimen NA3 (3.0 g) and specimen NA4, but closer or similar to NA3. However, because there are no aerogel particles in the control nonwoven fabric (Fig. 4b), the control specimen adsorbed the least amount of chemicals by the fibres (Fig. 4d). On the other hand, the surface of the aerogel–nonwoven fabric (NA4) was fully covered by the aerogel particles (4c). The aerogels create a barrier resisting the chemicals penetration through the fabric by adsorbing and holding the liquids in the pores of the particles. As a result, the dimension of the particles increased due to swelling, as shown in Fig. 4e. Once the aerogel particles became saturated after liquid adsorption, the chemicals would penetrate through the fabric similar to NC.

It was reported that the liquid adsorption process of adsorbents was mostly influenced by the size of pores and their distribution, the surface area along with pore surface chemistry [9]. As discussed earlier, silica aerogel is a highly porous material with pore size ranging from 5 to 100 nm, and the arrangement of the silica aerogel pore network is an open structure having interconnectivity with each other. Therefore, liquid chemicals are allowed to flow from one pore to another via the open-pore network with limited restriction [16]. This process permitted to adsorb

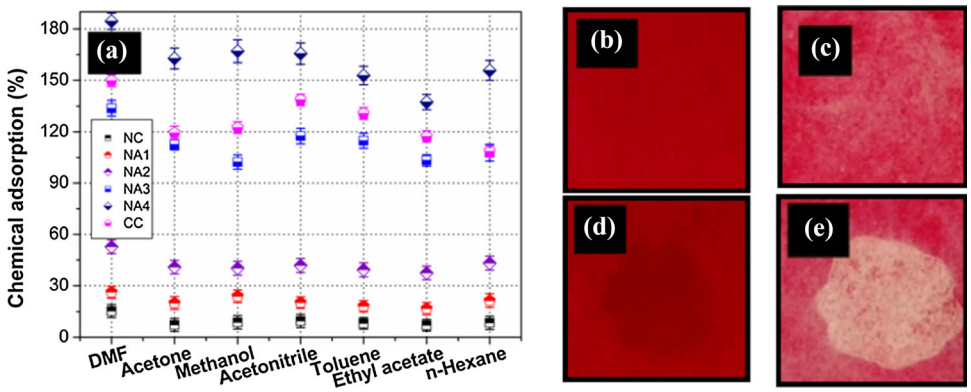


**Figure 4** Liquid chemical adsorption by the test specimens: **a** improvement of fabric chemical adsorption with aerogel concentrations; the inner surface layer of fabric (NC and NA4): **b** and **c** before and **d** and **e** after liquid adsorption.

more chemicals, consequently more chemical protection with the increment of aerogel concentration. In addition, the varying amount of liquid adsorption of different chemicals for the same fabric was due to the surface tension of the liquids as well as their density and volatility.

## Resistance to chemical penetration

The chemical resistance exhibited by the fabrics through adsorption of liquid and no chemical was retained on the surface of the fabrics. Therefore, all the specimens exhibited repellency of zero (0%) against all the liquid chemicals. Among the fabrics, the control nonwoven specimen demonstrated the minimum resistance against liquid penetration. In the penetration process, most of the liquid was adsorbed initially before penetrating through the fabric.

Commercial and aerogel–fabric NA3 and NA4 exhibited the greatest chemical resistance by retaining maximum amounts of liquids (Fig. 5a). The presence of a higher number of aerogel particles in the fabric facilitates the adsorption of a greater amount of liquid chemicals, which has been discussed earlier. Therefore, the resistance against liquid chemical penetration through the fabric increases as the increment of aerogel concentration and penetration of liquids through the fabric was not observed during the experimental investigation (Fig. 5b).

Chemical protection can be achieved through physical and chemical methods, for example, through formation an impermeable surface on fabric by laminating or coating. These coated fabrics have low surface energy and may display self-cleaning properties owing to the lotus effect, to resist the penetration of water and liquid chemicals. However, this impermeable clothing is usually impervious in both directions, and perspiration is unable to evaporate from the skin, creating heat stress for the user. Therefore, permeable protective clothing based on porous materials like activated carbon has been developed and used commercially. Such protective clothing system provides the chemical protection through liquid adsorption. The liquid adsorption concerning the chemical protection is mainly influenced by the porosity and the pore size of the activated carbon. As silica aerogels are more porous than activated carbon, the clothing system based on the porous silica aerogels will improve chemical protection.

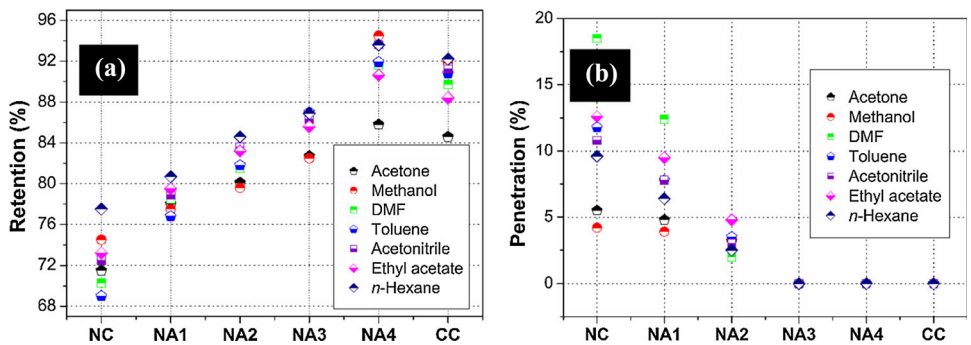


**Figure 5** Chemical resistance concerning **a** retention and **b** penetration of liquids.

## Resistance to dry heat transfer

Thermal resistance of fabric represents the ability of dry heat transfer through the clothing by conduction, convection, and radiation [27]. The transfer of metabolic body heat to the surroundings as well as radiant heat from the environment to the body is hindered due to the thermal resistance of the fabric. Therefore, thermal resistance is considered one of the important parameters to estimate the biophysical characteristics of clothing employed for various special purposes.

The resistance to dry heat transfer ($R_{cf}$) demonstrated by the fabric specimens is shown in Fig. 6. The commercial fabric showed the lowest dry heat resistance among all the specimens. For nonwoven fabric, a linear increase in dry heat resistance with increasing aerogel concentration was found for the aerogel–nonwoven specimens (Fig. 6). The thermal resistance of clothing depends on the structure and thickness of fabric as well as the thermal conductivity of the component fibres [26]. The increase in cloth thickness (Fig. 3) after incorporating aerogel particles was expected to increase the thermal resistance of the fabric. Besides, silica aerogels are highly porous material with very low thermal conductivity. The low thermal conductivity of aerogel contributed to a further increase in dry heat resistance by decreasing the overall thermal conductivity of the nonwoven specimens.

The thermal resistance of aerogel–nonwoven fabrics has also been assessed by employing an infrared thermal camera. The infrared thermography images in Fig. 7 demonstrate how quickly the heat transferred through the fabric samples when exposed to the same thermal condition, and all the specimens exhibit an increasing trend of temperature with time. The commercial fabric demonstrated a sharp rise in temperature with time: 23.3 °C, 29.1 °C, and 29.9 °C in 1 s, 45 s, and 90 s, respectively. Compared with the commercial fabric, a slow increase in temperature (23.4 °C, 27.5 °C, and 28.7 °C in 1 s, 45 s, and 90 s, respectively) was observed for the control nonwoven fabric. However, aerogel–nonwoven specimen (NA4) exhibited much slower increase in temperature (23.3 °C, 26.8 °C, and 27.7 °C for 1 s, 45 s, and 90 s, respectively), indicating that the fabric has the greatest thermal resistance among the specimens. Due to high thermal resistance, the aerogel–nonwoven fabrics will act as an insulating material by hindering the transfer of dry heat from the atmosphere towards the human body and vice versa. Therefore, the aerogel–fabrics can be utilized to protect the body by insulating the radiant heat from the environment or any other external hot source.

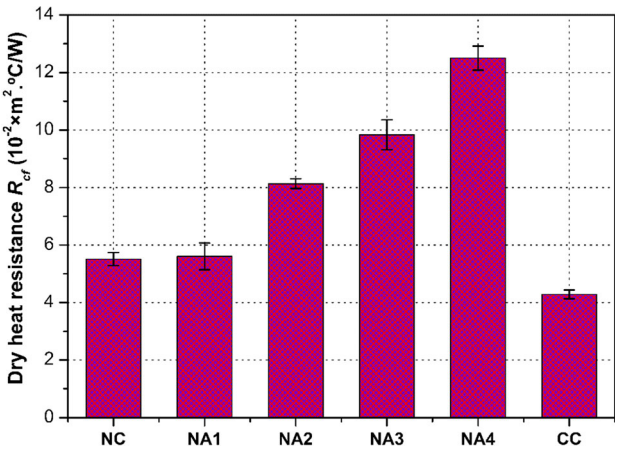


**Figure 6** Thermal resistance of fabric before and after aerogel incorporation.

## Radiant heat resistance

The time–temperature curves in Fig. 8 show the comparative performance of all the fabrics exposed to a radiant heat source. The rise of temperature up to 55 °C was considered as the endpoint of the test as this is the temperature when human skin received an irreversible second-degree burn [23]. In addition, the time to reach the pain threshold (44 °C) and the escape time, i.e., the time gap between feeling pain (44 °C) and receiving burn (55 °C) [24], was recorded to analyse and compare the radiative heat resistance of the nonwoven fabric specimens.

From Fig. 8, it is certain that radiative heat resistance of the developed aerogel–fabric has gradually increased with the increment of aerogel concentration in their nonwoven structure. The nonwoven fabric without aerogel (NC) reached the pain threshold (44 °C) within 192 s of heat exposure, whereas the maximum time (340 s) was recorded for the fabric having 4.0 g aerogels (NA4) to reach the pain threshold. Similarly, NA4 demonstrated the highest time to reach the second-degree burn temperature (55 °C) among all the fabrics. On the other hand, commercial protective clothing (CC) exhibited better performance than the fabrics NC and NA1 but showed significantly lower resistance compared with the specimens NA2, NA3, and NA3. The greater heat

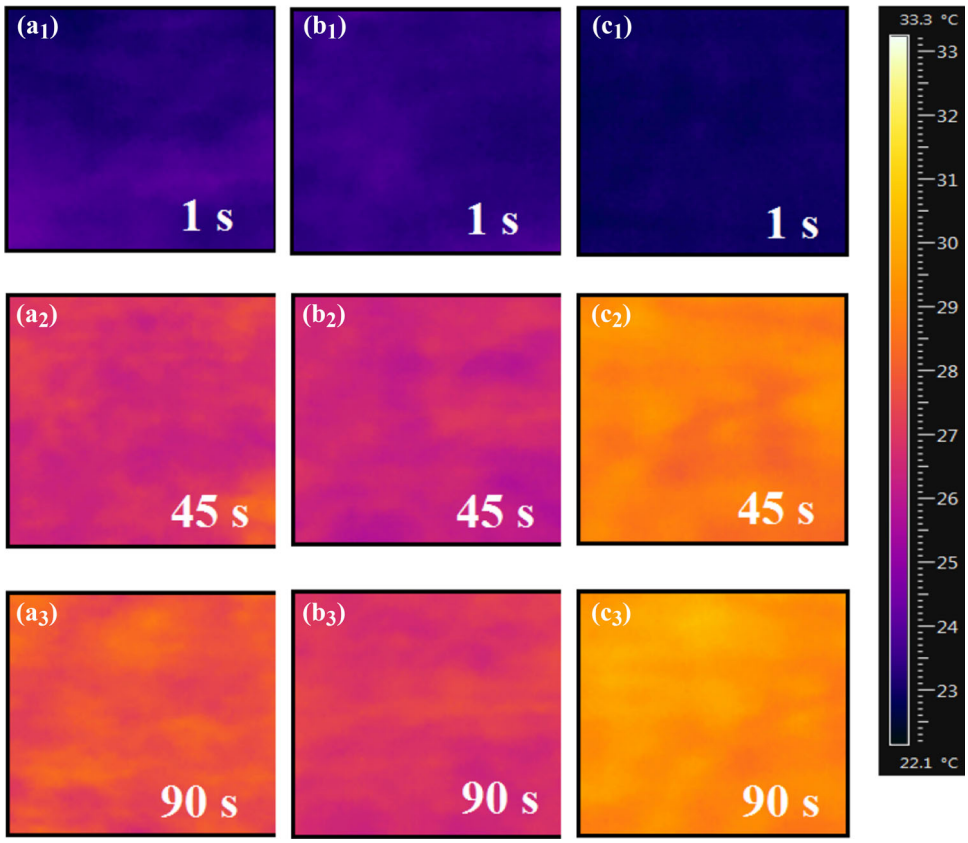


**Figure 7** Infrared thermography images of **a** control nonwoven, **b** aerogel–nonwoven (NA4), and **c** commercial fabric with time.

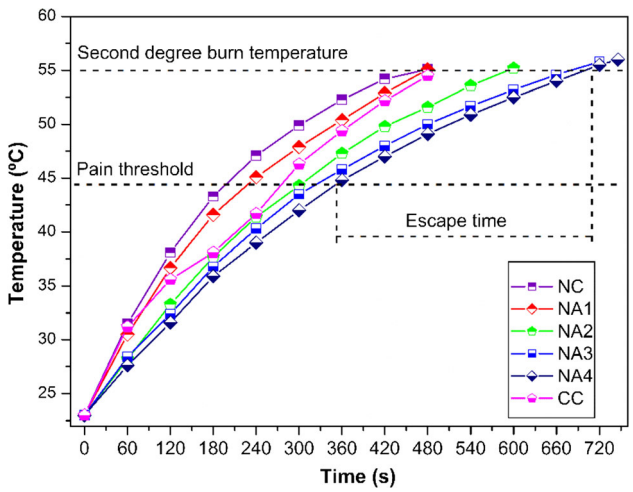


**Figure 8** Development of fabric radiative heat resistance.

resistance of aerogel fabrics was due to the low thermal conductivity of silica aerogel particles as well as the increased thickness of nonwoven fabrics, as mentioned earlier. This improved heat resistance of aerogel–nonwoven fabric can be employed to protect the body from the external source of radiant heat along with creating scope to avoid injury because of extended escape time.

## Air permeability of fabric

The air permeability of textile material is considered as a fundamental fabric characteristic determining the clothing comfort [28]. Generally, fabric hinders the flow of air from the human body to the atmosphere while wearing, and thus, fabric permeability to air is commonly used in estimating the 'breathability' of clothing ensembles employed for several special purposes [29].

Figure 9 shows that the commercial protective clothing demonstrated the highest permeability to air (53.88 mL $cm^{-2}$ $s^{-1}$) among the test specimens. Similar air permeability (50.83 mL $cm^{-2}$ $s^{-1}$) was exhibited by the control nonwoven fabric. The permeability of the specimens having aerogel particles decreases with the increment of aerogel concentrations. The breathability of nonwoven textiles is mostly influenced by the fabric structure, i.e., the openness or density of the cloth [30]. Hence, the increase in fabric density and reduction in openness due to aerogel particles among the fibres reduced the overall air permeability of aerogel–nonwoven specimens. The further reduction in porosity for the higher

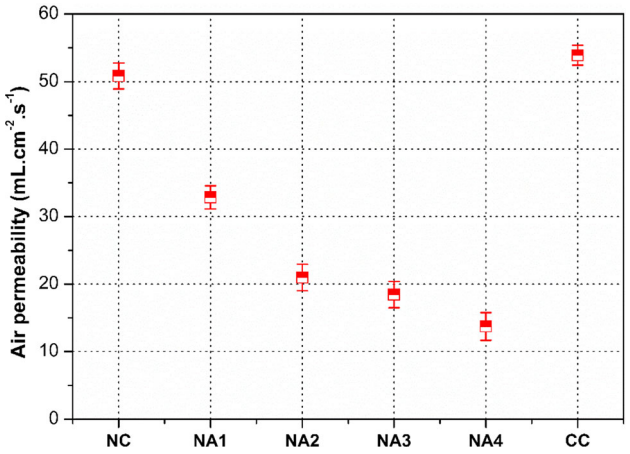


**Figure 9** Air permeability of fabric specimens at a pressure of 100 Pa.

aerogel content fabrics was due to the continuous layer of particles that hindered the flow of air by blocking the pores in the fabric. Consequently, an apparent declining of breathability can be observed in Fig. 9 for the fabric with more aerogel particles. Nevertheless, the breathability of fabrics (NA3 = 18.44 and NA4 = 13.72 mL cm$^{-2}$ s$^{-1}$ at 100 Pa) was still significantly high compared with the air permeability of various chemical protective clothing that was discussed in several contemporary research studies [16, 31, 32]. This high permeable protective fabric can be employed to facilitate the exchange of sufficient air to improve the apparel–skin microenvironment and provide adequate comfort along with consistent chemical protection.

## Evaporative heat transfer and permeability index

Evaporative heat transfer refers to how well the fabric can evaporate the body sweat to the environment through the clothing assembly [23]. Lower vapour transmittance specifies higher resistance to evaporative heat loss and vice versa. The high evaporative resistance of clothing hinders the flow of moisture vapour from the body and may create heat stress for the user in hot and humid condition. Moisture permeability index ($i_{mt}$) is an important parameter expressing the relationship between thermal and evaporative heat resistance of fabric [26]. This term is commonly used to determine how quickly the sweat vapour would be evaporated through the clothing.

Control nonwoven fabric demonstrated the minimum resistance against the vapour transmittance within the $R_{ef}$ range of 0–6 (Table 3), suggesting its efficient comfortability at the higher activity rate due to the extreme breathability. Comparable vapour resistance can be seen for the commercial fabric and aerogel–nonwoven fabric with the lowest concentration (NA1). However, aerogel-incorporated fabrics with higher aerogel particle concentration demonstrated a slightly elevated evaporative resistance (Fig. 10), but within the rating range of 6–13 (efficient or good comfortable at the moderate activity rate). This was due to the increase in fabric thickness as well as the layer of aerogel particles in the fabric that reduced the overall porosity of the fabric. Nevertheless, the average vapour resistance of the aerogel-incorporated fabrics (NA2 = 7.60; NA3 = 8.29; NA4 = 8.89 Pa m$^2$/W) did not increase much, and the values were very close to the lower limit of the $R_{ef}$ rating 6–13. Such small changes suggest that the fabrics were sufficiently permeable to moisture vapour with adequate breathability which will provide thermal comfort satisfactorily at the moderate activity rate and to some extent at the higher activity rate.

In the case of moisture permeability index ($i_{mt}$), however, nonwoven fabrics demonstrated a greater moisture permeability index compared with their commercial counterpart. The fabric having the maximum aerogel concentration (NA4) had the highest value (0.852) of moisture permeability index. The commercial fabric had an inferior value, a permeability index of 0.429. As mentioned earlier, the moisture permeability index is the ratio of thermal and evaporative heat resistance of the fabric. Though a greater resistance to evaporative transmittance was observed after adding aerogel particles (Fig. 10), practically a higher proportionate of increase in dry heat resistance (Fig. 6) to the vapour resistance enhanced moisture permeability index of aerogel–fabrics. The improved evaporative cooling index suggests that the fabrics will keep the body cool by shielding from the atmospheric radiant heat, and thus be able to manage favourable thermal comfort within apparel–skin microclimate in the hot environment.

**Table 3** Performance ratings of the fabrics based on evaporative resistance [26]

| $R_{ef}$ range (Pa m$^2$/W) | Performance | Test fabric rating |
|---|---|---|
| 0–6 | Very good or extremely permeable, comfortable at higher activity rate | NC, NA1, CC |
| 6–13 | Very good permeable. Comfortable at moderate activity rate | NA2, NA3 & NA4 |
| 13–20 | Acceptable permeability, not comfortable at high activity rate | |
| 20–30 | Unsatisfactory or slightly permeable, moderate comfort at low activity rate | |
| 30$^+$ | Insufficient permeable, not comfortable and short tolerance time | |

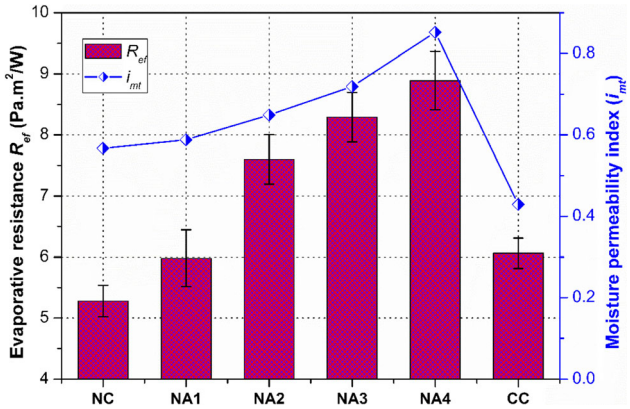


**Figure 10** Moisture permeability index ($i_{mt}$) and evaporative heat resistance ($R_{ef}$) of fabrics.

## Water uptake and evaporation rate of fabric

Water uptake of the fabric indicates the ability of absorbing liquid perspiration from the body, and the evaporation rate specifies how easily this perspiration can be vaporized to the atmosphere through the fabric. The water uptake and the evaporation rate are two common parameters generally used to determine the clothing comfort relating to the wet clinginess.

Table 4 shows that both control and aerogel-integrated fabrics can retain from 647 to 985% water on their conditioned weight, which is several times higher than the water uptake of commercial fabric (175%). The higher amount of water uptake by the nonwoven fabrics was due to the presence of viscose fibre, which is highly absorbent. Besides, the nonwoven fabric itself enhanced the water absorbency by allowing some water in their interstitial space of the less compact structure.

The change of fabric water content with time because of evaporation is shown in Fig. 11. Both the control and the aerogel–nonwoven fabrics retained a substantial amount of water after padding. The drying rate of both the commercial and nonwoven fabrics was analogous, and all the fabric specimens demonstrated a constant rate of evaporation with time (Fig. 11). The commercial fabric retained the least amount of water after padding and lost the water after 240 min, which was faster compared with the nonwoven fabrics (540 min). Nonwoven fabrics dried slower compared with the commercial counterpart because nonwoven fabrics held a larger amount of water. The higher water retention capability suggests that the nonwoven fabrics can retain larger amounts of body perspiration, which can be evaporated as water vapour to the atmosphere. Accordingly, the use of such fabric in protective clothing next-to-skin layer can be employed for chemical and thermal protection without undermining the clothing comfort concerning the wet clinginess in the higher activity level.

**Table 4** Water uptake (%) of the test fabrics at standard atmospheric condition

| Parameter | Test fabric specimen | | | | | |
|---|---|---|---|---|---|---|
| | NC | NA1 | NA2 | NA3 | NA4 | CC |
| Conditioned weight (g) | 1.76 | 2.05 | 2.55 | 2.70 | 2.77 | 4.0 |
| Saturated weight (g) | 19.1 | 19.8 | 20.5 | 20.3 | 20.7 | 11.0 |
| Water uptake (%) | 985.2 | 865.8 | 703.9 | 651.8 | 647.2 | 175.0 |

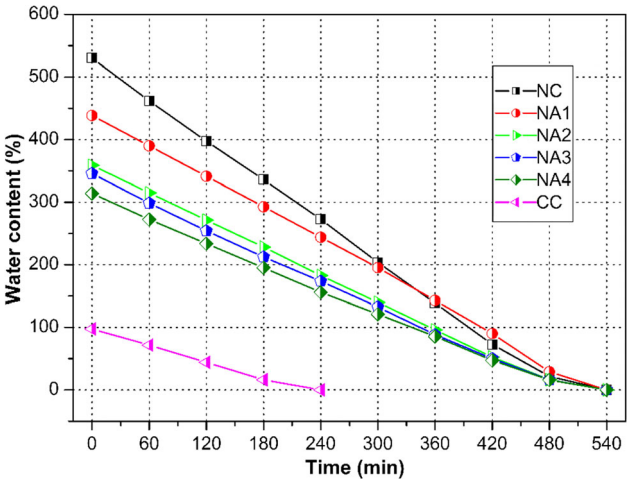


**Figure 11** Reduction in water content of fabric with time due to evaporation.

## Conclusions

Silica aerogel-integrated breathable nonwoven fabrics have been designed and developed for simultaneous chemical and thermal protection. The morphological analysis of the aerogel–fabrics revealed a layer of randomly distributed aerogel particles among the fibres. The aerogel particle layer can be utilized to provide effective chemical and heat protection. The aerogel–nonwoven fabrics are lightweight, though the addition of aerogel particles increased the fabric thickness. The fabrics after incorporating the aerogels exhibited improved chemical resistance, and as aerogel concentration increases, fabrics adsorbed more liquid chemicals. The increased thermal resistance of aerogel–fabrics suggested the body can be shielded from any external heat source. In view of thermophysiological wear comfort, the high air permeability of the nonwoven specimens indicated the exchange of sufficient air through the clothing to provide adequate breathability and thermal comfort. Besides, the improved evaporative transmittance and permeability index signified a favourable clothing comfort can be created more rapidly within apparel–skin microclimate in the hot and humid condition. In addition, the high water uptake and evaporation rate indicated that the nonwoven specimens can retain large amounts of body sweat as well as effectively evaporate the sweat into the atmosphere to provide clothing comfort concerning the wet clinginess. Thus, silica aerogel-integrated nonwoven interlining can be considered as a prospective material for developing protective clothing having reliable chemical and thermal protection along with breathability for wear comfort. Consequently, any deleterious effects because of heat stress can be mitigated considerably for the higher activity level of any emergency operation in a hot and humid atmosphere.

## Authors' contribution

MARB contributed to conceptualization, methodology, formal analysis, investigation, writing original draft. LW contributed to supervision, experimental design, review and editing. AS and IJ contributed to experimental investigation and data analysis. RAS contributed to review and editing. All authors discussed the results and contributed to the final manuscript.

## Funding

The authors disclosed no financial support for the research, authorship, and/or publication of this article. M. A. Rahman Bhuiyan is thankful to RMIT University, Australia, for scholarship support towards his PhD study.

## Compliance with ethical standards

**Conflict of interest** The authors declared no potential conflicts of interest with respect to the research, authorship, and/or publication of this article.

## References

[1] Yu Y, Wu X, Fang J (2015) Superhydrophobic and superoleophilic "sponge-like" aerogels for oil/water separation. J Mater Sci 50(15):5115–5124. https://doi.org/10.1007/s10853-015-9034-9

[2] Shaid A (2018) Incorporation of aerogel and phase change material in textiles for thermal protection. RMIT University, Melbourne, p 204

[3] Dorcheh AS, Abbasi M (2008) Silica aerogel; synthesis, properties and characterization. J Mater Process Technol 199(1–3):10–26

[4] Amonette JE, Matyáš J (2017) Functionalized silica aerogels for gas-phase purification, sensing, and catalysis: a review. Microporous Mesoporous Mater 250:100–119
[5] Venkataraman M et al (2018) Electrospun nanofibrous membranes embedded with aerogel for advanced thermal and transport properties. Polym Adv Technol 29(10):2583–2592
[6] Feng J et al (2016) Silica–cellulose hybrid aerogels for thermal and acoustic insulation applications. Colloids Surf A 506:298–305
[7] Hrubesh L, Keene L, Latorre V (1993) Dielectric properties of aerogels. J Mater Res 8(7):1736–1741
[8] Chen-Yang Y et al (2008) Influence of silica aerogel on the properties of polyethylene oxide-based nanocomposite polymer electrolytes for lithium battery. J Power Sour 182(1):340–348
[9] Štandeker S, Novak Z, Knez Ž (2007) Adsorption of toxic organic compounds from water with hydrophobic silica aerogels. J Colloid Interface Sci 310(2):362–368
[10] Xiong X et al (2018) Thermal and compression characteristics of aerogel-encapsulated textiles. J Ind Text 47(8):1998–2013
[11] Höffele S, Russell SJ, Brook DB (2005) Light-weight nonwoven thermal protection fabrics containing nanostructured materials. Int Nonwovens J 14(4):10–16
[12] Shaid A, Fergusson M, Wang L (2014) Thermophysiological comfort analysis of aerogel nanoparticle incorporated fabric for fire fighter's protective clothing. Chem Mater Eng 2(2):37–43
[13] Venkataraman M et al (2015) Novel techniques to analyse thermal performance of aerogel-treated blankets under extreme temperatures. J Text Inst 106(7):736–747
[14] Jin L, Hong K, Yoon K (2013) Effect of aerogel on thermal protective performance of firefighter clothing. J Fiber Bioeng Inf 6(3):315–324
[15] Shaid A, Wang L, Padhye R (2016) The thermal protection and comfort properties of aerogel and PCM-coated fabric for firefighter garment. J Ind Text 45(4):611–625
[16] Bhuiyan MR et al (2019) Polyurethane-aerogel incorporated coating on cotton fabric for chemical protection. Prog Org Coat 131:100–110
[17] Wilson A (2007) Development of the nonwovens industry. In: Russell SJ (ed) Handbook of nonwovens. Woodhead, Cambridge, pp 1–15
[18] Mao N, Russell S, Pourdeyhimi B (2007) Characterisation, testing and modelling of nonwoven fabrics. In: Russell S (ed) Handbook of nonwovens. Woodhead, Cambridge, pp 401–514
[19] Xiong X et al (2016) Transport properties of aerogel-based nanofibrous nonwoven fabrics. Fibers Polym 17(10):1709–1714
[20] Bhuiyan MAR et al (2019) Advances and applications of chemical protective clothing system. J Ind Text 49(1):97–138
[21] Bhuiyan MAR et al (2019) Polyurethane–superabsorbent polymer-coated cotton fabric for thermophysiological wear comfort. J Mater Sci 54(12):9267–9281. https://doi.org/10.1007/s10853-019-03495-8
[22] Mortan W, Hearle L (2008) Physical properties of textile fibers, 4th edn. Woodhead, Cambridge
[23] Shaid A et al (2018) Aerogel nonwoven as reinforcement and batting material for firefighter's protective clothing: a comparative study. J Sol-Gel Sci Technol 87(1):95–104
[24] Shaid A et al (2018) Effect of aerogel incorporation in PCM-containing thermal liner of firefighting garment. Cloth Text Res J 1–14
[25] Shaid A et al (2019) Low cost bench scale apparatus for measuring the thermal resistance of multilayered textile fabric against radiative and contact heat transfer. HardwareX 5
[26] Houshyar S et al (2015) Evaluation and improvement of thermo-physiological comfort properties of firefighters' protective clothing containing super absorbent materials. J Text Inst 106(12):1394–1402
[27] Nayak R et al (2018) Evaluation of thermal, moisture management and sensorial comfort properties of superabsorbent polyacrylate fabrics for the next-to-skin layer in firefighters' protective clothing. Text Res J 88(9):1077–1088
[28] Zupin Ž, Hladnik A, Dimitrovski K (2012) Prediction of one-layer woven fabrics air permeability using porosity parameters. Text Res J 82(2):117–128
[29] Saville B (1999) Physical testing of textiles, 1st edn. Woodhead, Cambridge
[30] Kothari VK, Newton A (1974) The air-permeability of nonwoven fabrics. J Text Inst 65(10):525–531
[31] Moiz A et al (2016) Chemical and water protective surface on cotton fabric by pad-knife-pad coating of WPU-PDMS-TMS. Cellulose 23(5):3377–3388
[32] Moiz A, Padhye R, Wang X (2017) Coating of TPU-PDMS-TMS on polycotton fabrics for versatile protection. Polymers 9(12):1–17